



Feasibility of artificial intelligence-based decision supporting system in tolvaptan prescription for autosomal dominant polycystic kidney disease

Jung Hyun Shin¹ , Ye Hyun Kim², Myung Kyu Lee², Hyun-Seok Min³, Hyungjoo Cho³, Hyunsuk Kim⁴,
Yong Chul Kim⁵, Yong Seong Lee⁶ , Tae Young Shin^{1,2}

¹Department of Urology, Ewha Womans University Mokdong Hospital, Seoul, ²Synergy A.I. Co., Ltd, Seoul, ³Tomocube Inc., Daejeon, ⁴Department of Nephrology, Hallym University Chuncheon Sacred Hospital, Chuncheon, ⁵Department of Nephrology, Seoul National University Hospital, Seoul, ⁶Department of Urology, Chung-Ang University Gwangmyeong Hospital, Gwangmyeong, Korea

Purpose: Total kidney volume (TKV) measurement is crucial for selecting treatment candidates in autosomal dominant polycystic kidney disease (ADPKD). We developed and investigated the performance of fully-automated 3D-volumetry model and applied it to software as a service (SaaS) for clinical support on tolvaptan prescription in ADPKD patients.

Materials and Methods: Computed tomography scans of ADPKD patients taken between January 2000 and June 2022 were acquired from seven institutions. The quality of the images was manually reviewed in advance. The acquired dataset was split into training, validation, and test datasets at a ratio of 8.5:1:0.5. Convolutional, neural network-based automatic segmentation model was trained to obtain 3D segment mask for TKV measurement. The algorithm consisted of three steps: data preprocessing, ADPKD area extraction, and post-processing. After performance validation with the Dice score, 3D-volumetry model was applied to SaaS which is based on Mayo imaging classification for ADPKD.

Results: A total of 753 cases with 95,117 slices were included. The differences between the ground-truth ADPKD kidney mask and the predicted ADPKD kidney mask were negligible, with intersection over union >0.95. The post-process filter successfully removed false alarms. The test-set performance was homogeneously equal and the Dice score of the model was 0.971; after post-processing, it improved to 0.979. The SaaS calculated TKV from uploaded Digital Imaging and Communications in Medicine images and classified patients according to height-adjusted TKV for age.

Conclusions: Our artificial intelligence-3D volumetry model exhibited effective, feasible, and non-inferior performance compared with that of human experts and successfully predicted the rapid ADPKD progressor.

Keywords: Artificial intelligence; Image processing, computer-assisted; Multidetector computed tomography; Polycystic kidney, autosomal dominant

This is an Open Access article distributed under the terms of the Creative Commons Attribution Non-Commercial License (<http://creativecommons.org/licenses/by-nc/4.0>) which permits unrestricted non-commercial use, distribution, and reproduction in any medium, provided the original work is properly cited.

Received: 30 December, 2022 • **Revised:** 12 March, 2023 • **Accepted:** 26 March, 2023 • **Published online:** 4 May, 2023

Corresponding Authors: Tae Young Shin <https://orcid.org/0000-0002-3910-9252>

Department of Urology, Ewha Womans University Mokdong Hospital, 1071 Anyangcheon-ro, Yangcheon-gu, Seoul 07985, Korea

TEL: +82-2-2650-5158, FAX: +82-2-2650-5154, E-mail: tyshin@ewha.ac.kr

Yong Seong Lee <https://orcid.org/0000-0003-0611-4554>

Department of Urology, Chung-Ang University Gwangmyeong Hospital, 110 Deokan-ro, Gwangmyeong 14353, Korea

Tel: +82-2-2610-6631, Fax: +82-2-2610-6630, E-mail: yongslee@cau.ac.kr

INTRODUCTION

Autosomal dominant polycystic kidney disease (ADPKD) is the most common hereditary and progressive disease with an average prevalence of 2.7 in 10,000 people. ADPKD accounts for approximately 10% of end-stage renal disease and is characterized by progressive, fluid-filled cyst formation originating from 1% to 2% of the nephrons [1]. The kidney gradually enlarges due to compensatory hyperfiltration in non-cystic nephrons and this renal hypertrophy results in pain, a palpable mass, hypertension, hematuria, cyst rupture, cyst infection, and ultimately, renal failure [2]. There has been no definite treatment for ADPKD until the 2010s, although tolvaptan, a vasopressin V2 receptor antagonist, has shown efficacy in reducing the annual increase in total kidney volume (TKV) and renal function deterioration [3]. TKV is an important parameter for predicting disease progression and has been suggested as a key prognostic factor to identify patients who are at risk of rapid progression to renal failure [4,5].

Traditionally, manual labeling of kidney contours on each computed tomography (CT) scan or magnetic resonance image (MRI) has been considered the most accurate TKV measurement system [6,7]. However, the entire process is laborious, time-consuming, and carries the risk of human error and interobserver discrepancy. Consequently, robust investigations of more efficacious and accurate tools for TKV calculation have been conducted. Numerous studies have reported the functional outcomes of semi-automated measurement and deep learning-based artificial intelligence (AI) volumetry in various image modalities, including CT, MRI, and ultrasound (US) [8]. We had previously developed an AI-based volumetry framework for polycystic kidney and liver diseases [9]. The performance of our AI was fast and accurate with outcomes that are highly comparable to those from human specialists. In the present study, we upgraded, trained, and applied our deep learning volumetry system to larger clinical datasets and investigated its performance on ADPKD patients. Next, we applied our AI-based volumetry to develop software as a service (SaaS) which is based on Mayo imaging classification to identify the ADPKD rapid progressors.

MATERIALS AND METHODS

1. Ethics and data availability statement

This study was approved by the Institutional Review Board (no. 2022-08-028) of the Ewha Womans University Mokdong Hospital, and informed consent was waived due

to the retrospective study design. In addition, current study was performed according to TRIPOD-AI reporting guideline. The reference source code for GitHub is follows: https://github.com/Project-MONAI/tutorials/tree/main/modules/dynunet_pipeline.

2. Dataset information and study population

We have established a polycystic kidney CT database, which includes both raw data and a hand-labeled, semantic-segmentation dataset inspected by experts [9]. ADPKD-related data were sorted from the existing raw data and additional CT images of ADPKD cases taken between January 2000 and June 2022 were acquired from seven hospitals under two medical centers. Patients undergoing dialysis at the time of the CT scan and those with any noisy data on CT scans were excluded. All images were manually reviewed by radiologists in advance. Pooled data from institutions were combined to construct a CT-ADPKD database.

3. Overview of the training process

The TKV calculation algorithm of our study extracts the ADPKD area by first analyzing the abdominopelvic CT images based on the well-trained, semantic-segmentation model named “3D Dynamic U-Net”, a type of convolutional neural network-based segmentation model. The AI segmentation model first undergoes a process of learning large amounts of data to transform and distinguish functional relationships of data consisting of pairs of a 3D CT array and a correct 3D CT Mask array. The overall workflow of the algorithm consists of three steps: data preprocessing, ADPKD area extraction, and post-processing. After going through all the processes of the algorithm, a 3D segment mask is obtained and TKV is calculated.

4. Preprocessing

The range of Hounsfield Unit values considered meaningful were clipped and converted to a float32 data type in the range of 0.0 to 1.0 so that the graphic process unit could accelerate it. Next, missing values were input, noisy data were smoothed, identified outliers were removed, and solvent data inconsistency was checked. The process of handling noisy data was replaced with an image preview by radiologists. In the case of patients with duplicated process IDs, only samples with non-overlapping series were included in the dataset.

5. ADPKD area extraction

We applied a network based on a 3D Dynamic U-Net for ADPKD segmentation. The model was provided by the

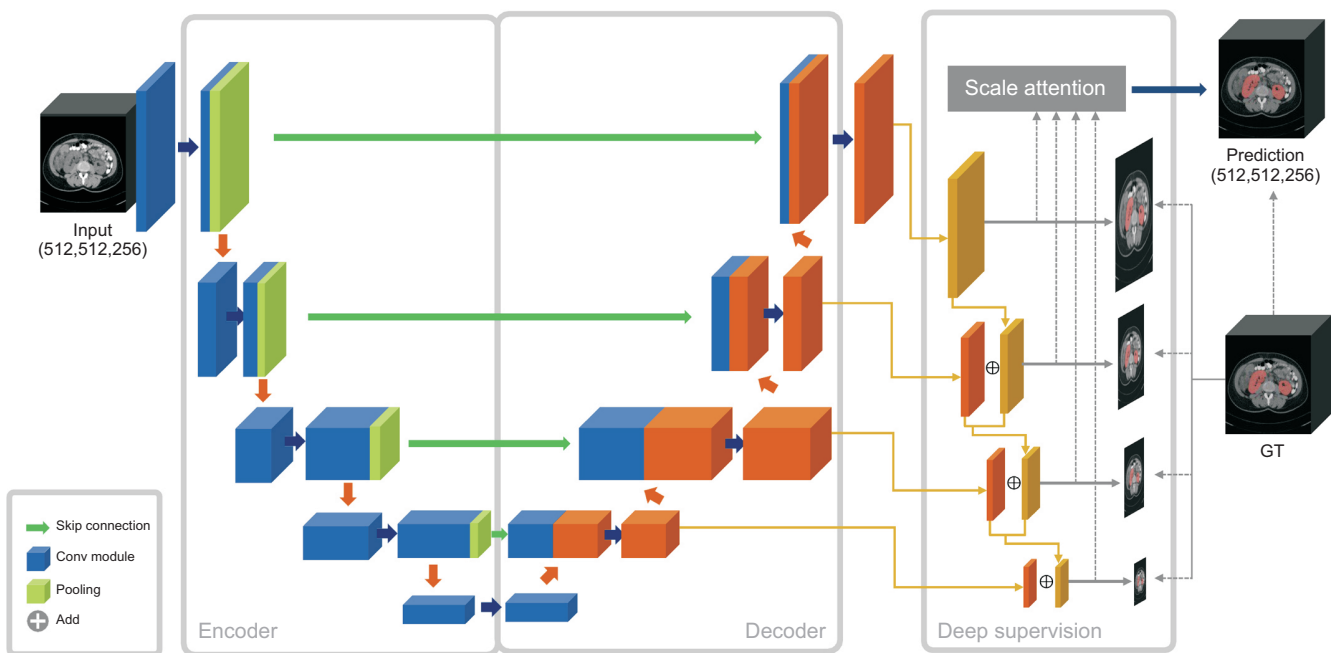


Fig. 1. Dynamic 3D U-net architecture. The model architecture used for 3D segmentation mask inference for autosomal dominant polycystic kidney disease total kidney volume calculation. Conv, convolutional; GT, ground-truth mask.

MONAI Project, which is an open-source project for the latest model baseline codes associated with medical AI (e.g., 3D Dynamic U-Net, 2D/3D Residual U-Net, and 3D UNetR). Either 2D or 3D arrays were input to 3D Dynamic U-Net, and residual block and deep supervision were applied for learning. Deep supervision calculates the final loss by multiplying each loss term by weight after calculating the loss between all featured maps and the ground-truth mask images (Fig. 1).

In addition, instance normalization was robustly applied to learn the heavy model, even in small batch sizes. To prevent 3D input data from causing out-of-memory problems, we split the input data into small 3D patches. In this process, 3D patches were extracted in a sliding window to prevent the occurrence of grid pattern artifacts in the segmentation mask inferred by the model. The batch size was set to 1 (one case), and the learning rate was set to decay according to $(1 - \text{epoch} / \text{max_epochs}) \times 0.9$, and training was performed for 220 epochs. Data augmentation was applied with the following settings:

- Random zoom: min_zoom 0.9, max_zoom 1.2 (15%)
- Random Gaussian noise: std 0.01 (15%)
- Random vertical flip (50%)

6. Post-processing

Area extractions performed by AI sometimes contain false-alarm cases with holes between slices. Although these false-alarm cases might not be a major problem in the TKV calculation, they should be removed during post-processing

as they negatively impact the overall quality of the 3D reconstruction. As the kidney should maintain a constant shape without breaking, the slice with a false alarm was interpolated and filled. The pseudo-code of the false-alarm removal algorithm was executed on both kidneys, and images were merged to obtain a 3D mask of the kidney with complete connectivity.

7. TKV calculation

The 3D mask volume was constructed using the inferred segmentation masks after completion of all the mentioned processes. TKV was calculated by applying the 3D volume to the volume calculation equation:

$$\text{TKV (mm}^3\text{)} = \text{pixel spacing (width, height)} \times \text{slice thickness (depth)} \times \text{total number of voxel}$$

The full flow chart of our algorithm is graphically summarized in Fig. 2.

8. Development of SaaS from AI-based kidney volumetry

After validation of our AI-based kidney volumetry, we developed SaaS (SYN-IGN-AN, Ignite™, Synergy A.I. Co. Ltd) to identify the rapid progressors among ADPKD patients. Mayo imaging classification is currently the best prediction model for selecting rapid progressors among ADPKD patients and is also a good predictor for Korean ADPKD population [10]. The SaaS included uploading of Digital Imaging and Communications in Medicine (DICOM) images for

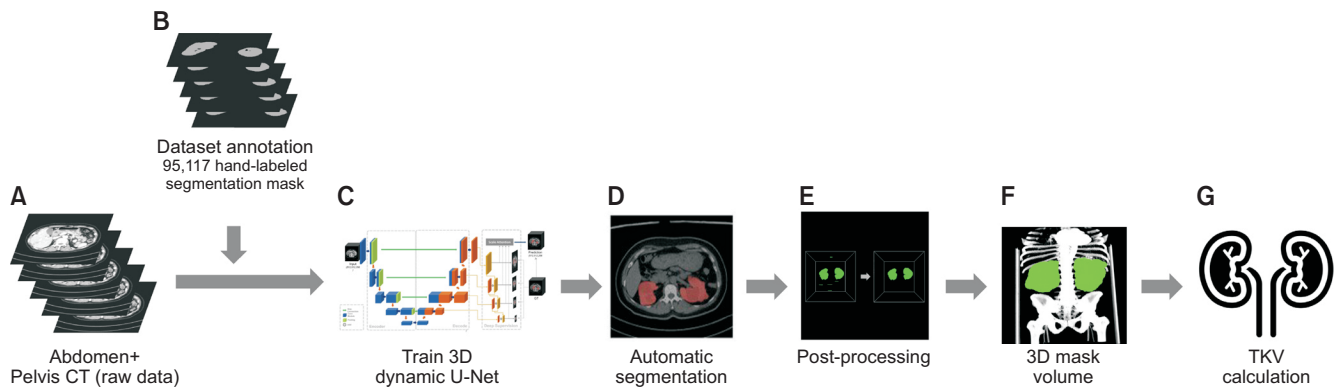


Fig. 2. Overall flow chart of the algorithm. (A) Abdomen and pelvis computed tomography (CT) images were acquired from several hospitals. (B) Dataset was annotated with hand-labelled segmentation mask. (C) 3D Dynamic U-net model was trained with the dataset, which was previously constructed with 38,261 hand-labeled semantic-segmentation and inspected by three expert radiologists. (D) Automatic segmentation was performed to test autosomal dominant polycystic kidney disease samples with the trained model. (E) Collected masks inferred by the model underwent post-processing to remove false alarms. (F) 3D volume model was constructed with inferred segmentation masks. (G) Total kidney volume (TKV) calculation was performed by applying the 3D volume to the volume calculation equation.

TKV measurement, and other variables including age, sex, race, height, serum creatinine, and genotype.

9. Statistical analysis

The acquired dataset was split into training, validation, and test data at a ratio of 85:1:0.5 to investigate the performance of the model. The pixel array shape of each DICOM file was $512 \times 512 \times S(n)$. To calibrate the discrepancy in the number of slices for each sample, padding filled with zeros was added to the cases with less than 250 slices.

To evaluate the performance of the medical image analysis algorithm, the dice similarity correlation (DSC) score was used as a statistical validation metric to assess the accuracy of spatial overlap between the true and predicted manual segmentation labels using the following formula:

$$\text{DSC} = \frac{2 \times \text{True Positive}}{(\text{True Negative} + \text{False Positive} + \text{True Positive} + \text{False Negative})}$$

Before calculation, the 3D masks of the kidney region were obtained from 32 test cases using a well-trained model (the number of slices may be different in each case). After the model inferred the 3D masks for 32 test samples, a confusion matrix was constructed and the DSC calculated. Five-fold cross-validation was performed to confirm the robustness of the model for the training dataset. The comparison between ground-truth and auto-segmented TKV was also performed with calculation of an interclass correlation coefficient (ICC).

RESULTS

1. Dataset information

A total of 753 cases with 95,117 slices were included in

the dataset. CT images were acquired from eight types of CT scanners in seven institutions. The average number of slices in the entire dataset was 126 (range 26–276). The model was trained with 655 CT-DICOM files with 82,850 slices, validated with 66 DICOM files with 7,778 slices, and tested with 32 DICOM files with 4,489 slices. The detailed information of our database is summarized in Table 1.

2. Performance of the algorithm

The differences between the ground-truth ADPKD kidney mask and the predicted ADPKD kidney were negligible (Fig. 3). The ICC calculated by comparing the ground truth and AI auto-segmentation TKV results was 0.99976, which is extremely reliable (Fig. 4). Most of the differences were false alarms, which were successfully removed by the post-process filter; as shown in Fig. 5, they had no clinical significance. The test-set performance plot shows homogeneously equal performance in each of the 32 test samples (Fig. 6).

The test DSC score of our model was 0.971 and the DSC score improved to 0.979 after post-processing (Table 2).

3. Operation of AI-based kidney volumetry

After dragging-and drop of DICOM files from the CT scan, patients' baseline demographics including age, sex, race, height, and serum creatinine is entered (Fig. 7A). After inference of the data, kidney volume is calculated automatically and ADPKD classification is reported (Fig. 7B). The overall process for using our SaaS is presented in Supplementary Video.

Table 1. Baseline information of participating hospitals, types of CT images, and the model names of the CT scanners

	Hospitals						Total		
	Hallym-Chuncheon	Hallym-Pyeongchon	Hallym-Kangdong	Hallym-Kangnam	Hallym-Dongtan	Ewha-Mokdong	Ewha-Seoul	Total DICOM	Total slice
Dataset (n)									
Noncontrast	27	54	41	37	23	156	128	753	95,117
Contrast	6	9	3	4	10	138	59		
Model name of the CT scanners	SOMATOM Definition Flash (Siemens)	SOMATOM Sensation 64 (Siemens) SOMATOM Definition Edge (Siemens) SOMATOM Definition Flash (Siemens)	SOMATOM Smile (Siemens) MX8000 IDT (Philips)	Brilliance CT 64-Channel (Philips) MX8000 IDT (Philips) SOMATOM Sensation 64 (Siemens)	Brilliance Big Bore (Philips)	SOMATOM Sensation 64 (Siemens)	SOMATOM Force (Siemens)	8 CT scanners 7 Institutions	

CT, computed tomography; DICOM, Digital Imaging and Communications in Medicine.

DISCUSSION

The Mayo imaging classification is a simple tool that can easily identify patients at the highest risk for disease progression regardless of renal function and is currently used for tolvaptan treatment candidate selection [11,12]. Accurate TKV measurement is crucial for prompt decision-making; however, TKV is generally approximated with ellipsoidal kidney length, width, and depth measurements due to the lack of feasible, commercialized, technical support. The present study focus on kidney volume only and presents the excellent performance of a well-trained, deep learning volumetry system, a 3D-Dynamic U-Net, in the largest clinical dataset, which can be helpful in overcoming the aforementioned drawbacks. Our AI model was fully automated and had a Dice score of 0.971, which was further improved to 0.979 by removing clinically insignificant data via post-processing. Moreover, our AI model was successfully applied to SaaS which is designed to identify rapid progressors.

Current studies on deep learning-based volume measurement in ADPKD utilize various image modalities, including CT scans, MRI, and US. The Dice score of each segmentation methodology ranges from 0.86 to 0.969 for CT scans [9,13,14] and 0.84 to 0.98 for MRIs [15-19]. There are few studies on US; one study by Jagtap et al. [20] reported a dice score of 0.80 by 2D U-Net segmentation in kidney US. Our 3D-Dynamic U-Net provided the highest Dice score of 0.971 compared to previous studies using CT scans. This excellent, expert-level performance is based on a large clinical dataset. Our dataset included 95,117 slices from 753 ADPKD patients, which is the largest number of study subjects reported so far.

Early deep learning-based methods usually consist of semi-automated systems in which AIs produce the initial prediction of renal contours that can later be confirmed and modified by radiologists [21,22]. Such a system omits the process of laborious manual drawing on each slide, resulting in time-cost effectiveness, efficiency, accuracy, and improved ergonomics for the physicians. However, a semi-automated system always requires expert manpower for supervision, and there is always a risk for human error. Volumetry, including TKV measurement, is a field of work that requires consistency and reproducibility. This has resulted in the need for semi-automated segmentation in order to overcome the limitations of manual annotation. Our AI model provides a fully automated segmentation technique with a Dice score of 0.979, which is non-inferior to human specialists who had DSC ranging from 0.957 to 0.975 based on our previous report [9].

Among various segmentation models, we chose 3D Dy-

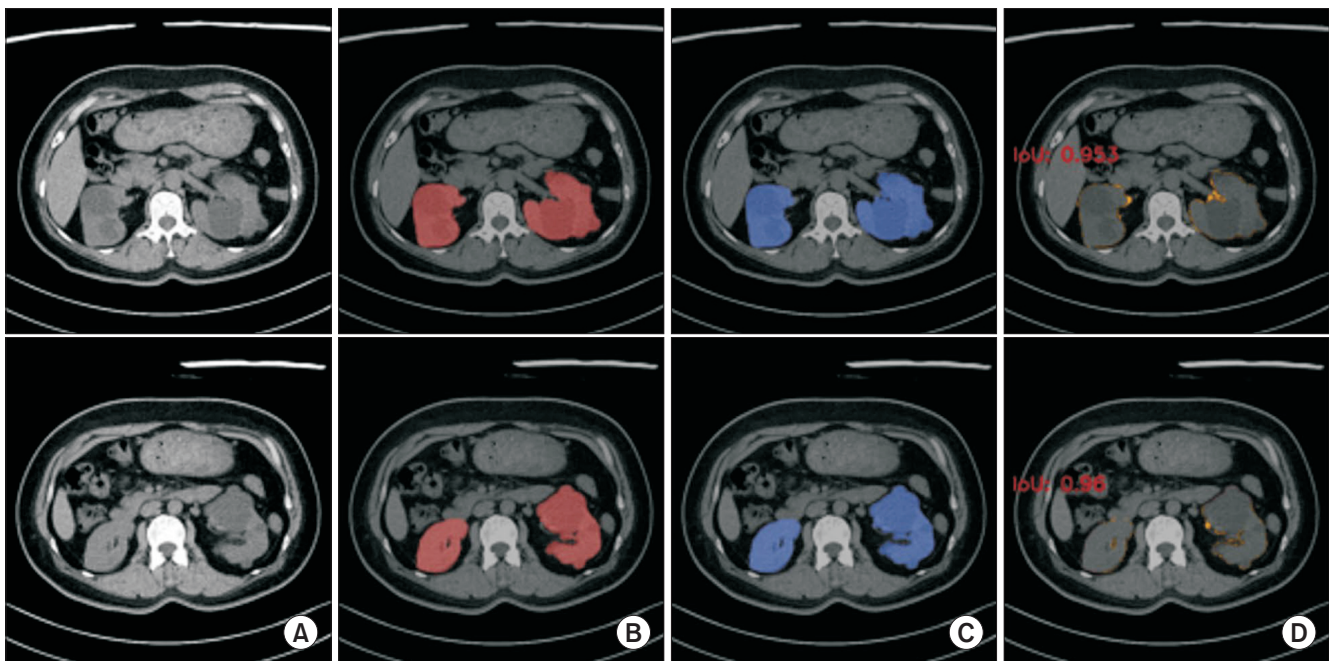


Fig. 3. Comparison between ground truth and artificial intelligence auto-segmentation. (A) Original computed tomography slice image. (B) Ground-truth mask image superimposed onto the original input image. (C) Predicted mask image superimposed onto the original image. (D) The differences between (B) and (C) relative to the original images. IoU, intersection over union.

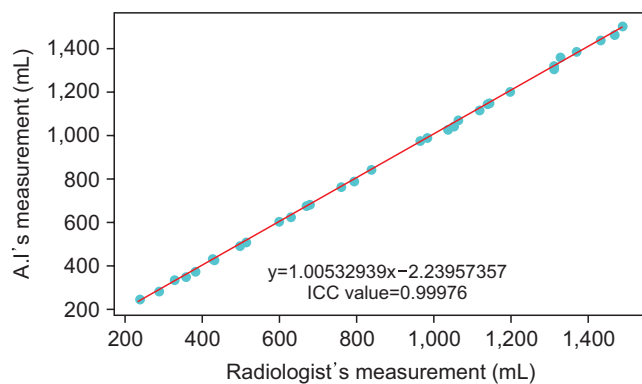


Fig. 4. The interclass correlation coefficient (ICC) between ground truth and artificial intelligence (AI) auto-segmentation.

dynamic U-Net as the main network of the present study rather than 2D/3D Residual U-Net, 3D-UnNetR, and the 3D-Dynamic U-Net 5-Fold ensemble set. Three-dimensional Dynamic U-Net is implemented based on the nnU-Net architecture proposed by Isensee et al. [23] and has three advantages compared to the general vanilla U-Net. First, residual connection is supported in convolutional blocks. Second, anisotropic kernel sizes and strides can be used in each layer. Third, deep supervision heads can be added. Moreover, 3D Dynamic U-Net generates full-resolution feature maps at multiple semantic levels owing to the nested skip pathways. Thus, the losses are estimated from four semantic levels. The deep supervision enables model pruning and improves, or in

the worst case, achieves comparable performance to using only one loss layer.

Our segmentation model includes an important refinement process named “post-processing”. Post-processing identifies and removes false alarms, which usually have no clinical significance, leading to an improvement of the Dice score in both validation and test sets. The differences between pre- and post-process filters might not be significant (0.971 vs. 0.979) as the performance of 3D-Dynamic U-Net itself is highly competitive. However, such processes should not be neglected as aesthetic mask quality improvement provides more accurate and reliable 3D images for both clinicians and patients. As a 3D printed model is commonly used to facilitate more intuitive explanation to patients, it is crucial that the quality of 3D images be reliable. This enables better understanding of patients regarding their clinical information and might lead to higher compliance and persistence rate to the clinicians.

Five years have passed since the approval of tolvaptan for kidney disease, but several problems remain unsolved in clinical practice. Efficacy monitoring of any newly adopted drug is necessary for objective and scientific evaluation. The therapeutic efficacy of tolvaptan is frequently monitored by changes in serum glomerular filtration rate (GFR) but not consecutive TKV measurements due to the absence of reliable methodologies in clinical practice [4].

Consecutive TKV measurements are important and help-

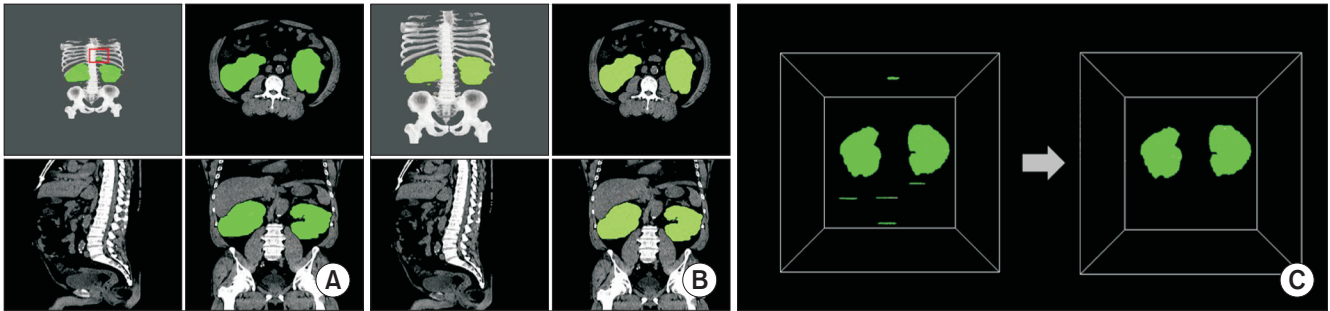


Fig. 5. Representative image of post-processing filter. (A) Before post-process filter application. (B) After post-process filter application. (C) Comparison of rendering 3D space before and after post-process filter.

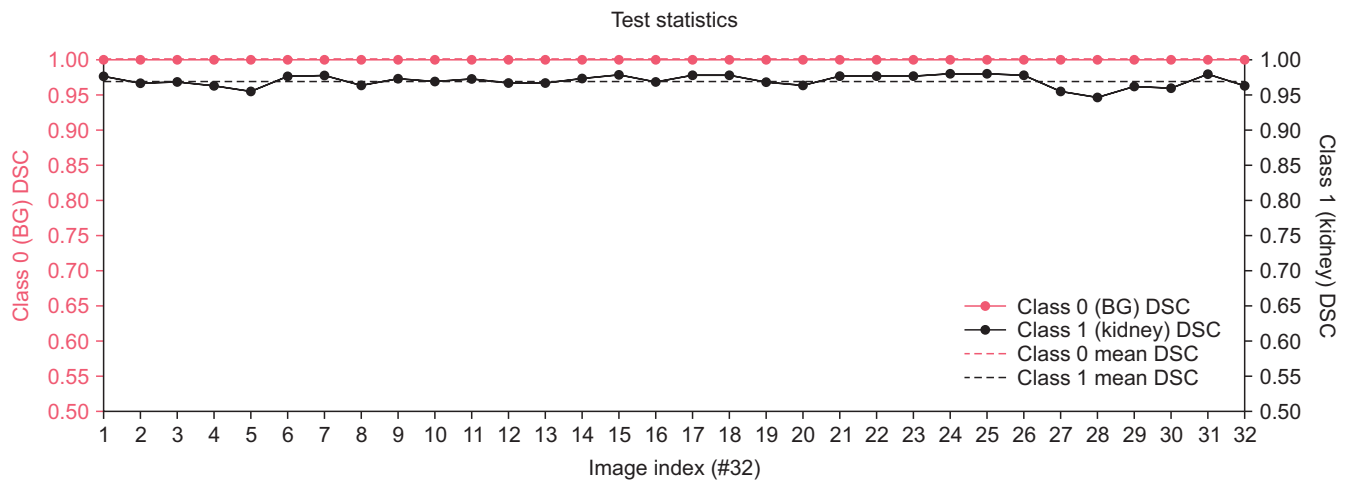


Fig. 6. Test set performance plot. The solid red line represents the dice similarity correlation (DSC) score of the background class for each test sample, and the solid black line represents the DSC score of the autosomal dominant polycystic kidney disease (ADPKD) kidney class for each test sample. The red and the black dotted lines denote the average DSC scores of the background class and the ADPKD kidney, respectively.

Table 2. Performance of the artificial intelligence auto-segmentation model

Model	Test Dice score	Validation Dice score
3D-Dynamic U-Net	0.971	0.967
After post-processing (for 3D model)	0.979	0.970

ful for treatment efficacy monitoring. First, there are other comorbidities, including uncontrolled hypertension, diabetes, and vascular disease, which could be modifiable contributing factors for GFR decline in ADPKD patients [24,25]. Serial TKV monitoring is necessary to confirm that renal function deterioration is actually due to ADPKD progression. Second, there is still no definite titration regimen for tolvaptan associated with maximal therapeutic efficacy and minimal adverse events [4,26]. The combination of GFR and TKV on serial follow-ups might be useful to precisely determine the effects of tolvaptan persistence on the clinical course of ADPKD. This, in turn, could lead to the establishment of a clear treatment strategy. Third, tolvaptan is currently the only

drug being widely prescribed for ADPKD and is extremely expensive. Patients need to take the medication twice a day until they progress to end-stage renal disease. The duration of treatment could be a lifetime if the side effects [27,28] (especially liver toxicity and polyuria) are tolerable and renal function is maintained. This is a serious socio-economic burden for both the affected individuals and society. Hence, it is very important to provide scientific evidence to decide which types of patients should get medical expense coverage for tolvaptan usage.

Despite the need for sufficient research on TKV measurement, there are few 3D volumetry techniques capable of effective and accurate calculation. Variations in image modalities, models, protocols, and the performance of radiologists were considered insurmountable in traditional settings. Moreover, valid and sensitive approaches for monitoring the changes in TKV have not yet been established. Our AI 3D-volumetry could be a breakthrough for such problems as it is capable of high-quality performance in datasets where most images are non-enhanced CT scans, which do not re-

Task

Click to attach files
Only DICOM folder allowed

Drag and Drop To attach files
Only DICOM files or Zip file allowed

(187)

EWHA_ADPKD053adam X
EWHA_ADPKD052adam X
EWHA_ADPKD053adam X
EWHA_ADPKD057adam X
EWHA_ADPKD056adam X
EWHA_ADPKD054adam X
EWHA_ADPKD055adam X
EWHA_ADPKD054adam X

KIM ****G HAK 29Y

M 87.6

Patient height(cm) yyyy/mm/dd

Serum Creatinine(mg/dL) -- choose option --

Hypertension before 35P YES NO

Urological event before 35P YES NO

African American YES NO

Family members with ESRD? YES NO

UPLOAD

ANALYSIS REPORT

General Information

Selected Patient: KIM ****G HAK

Age/Gender: 29/M

Height/Weight (cm/kg): 183/87.6

Race (African or not African): 0

Serum creatinine (mg/dL): 2

eGFR (ml/min/1.73m²): 40.30

Mutation: truncating

Hypertension before 35P: No

Urological event before 35P: No

TKV (ml/m): 850.75

HTKv (ml/m): 185.90

PKDHD score: 5

RECOMMEND: 500 median age for 35SD onset

ADPKD classification

Prediction of future eGFR based on Classification

Future Time (years)

If you enter a Future Time, you will get the predicted kidney function for that time.

Fig. 7. Representative process for utilizing Ignites. (A) Default page for patient information input. Digital Imaging and Communications in Medicine (DICOM) files for kidney volume calculation can be uploaded. Patient demographics including age, weight, height, serum creatinine, and autosomal dominant polycystic kidney disease (ADPKD) genotypes are entered for ADPKD classification. (B) ADPKD classification of the selected patient.

quire any special protocol (although radiation exposure dose and image thickness might differ).

The limitations of the present study are as follows. We needed a training dataset created by experts to set ground-truth images and this dataset only included CT scans. However, there is no other way for setting ground-truth images except for hand-labeled semantic segmentation. In addition, CT scan is more favorable than MRI as setting a ground-truth value in low-resolution MRI is extremely difficult to be generalized based on differences in vendor and hospital setting values. Our AI volumetry presented high-quality performance despite the use of non-enhanced CT scans.

We report an automatic 3D-volumetry model from various CT models by using the largest clinical dataset reported to date; this successfully reflects the heterogeneity of real-world settings. Furthermore, post-processing of the predicted 3D images improved image quality with better aesthetics, accuracy, and reliability. Furthermore, we developed SaaS based on Mayo imaging classification to support clinical decision on tolvaptan prescription.

Tolvaptan is the only Food and Drug Administration-approved drug for ADPKD treatment. However, currently available studies are mostly clinical trials on ADPKD patients who were mostly recruited from Western countries; therefore, robust investigations on other ethnicities and studies that reflect real-world data are urgently required. Above all, future studies should utilize more comprehensive clinical data by including not only serum GFR but also TKV. If our AI-based segmentation model is more widely applied to real practice, non-inferior and high-quality data could be provided to both physicians and patients without laborious and time-consuming, manual labeling by radiologists. In addition, further clinical decision-making, including

therapeutic outcome monitoring, and prediction of prognosis, might be more efficacious, leading to decreased medical expenses. Future studies with external validation and comparison with other segmentation models are warranted for the clinical application of this outstanding AI volumetry technique in real-world settings.

CONCLUSIONS

Our deep learning-based, automatic-segmentation, 3D volumetry exhibited effective, feasible, and non-inferior performance compared with that of human experts. This model was improved by post-processing to provide more accurate and reliable 3D images for both clinicians and patients. Moreover, application of AI 3D-volumetry to SaaS for selecting rapid progressors was also successful.

CONFLICTS OF INTEREST

The authors have nothing to disclose.

FUNDING

This work was supported by the Starting growth Technological R&D Program (TIPS Program, no. S3079853) funded by the Ministry of SMEs and Startups (MSS, Korea) in 2021, and Institute of Information & communications Technology Planning & Evaluation (IITP) grant funded by the Korea government (MSIT) (No.RS-2022-00155966, Artificial Intelligence Convergence Innovation Human Resources Development [Ewha Womans University]).

AUTHORS' CONTRIBUTIONS

Research conception and design: Yong Seong Lee and Tae Young Shin. Data acquisition: Ye Hyun Kim, Myung Kyu Lee, Hyun-Seok Min, and Hyungjoo Cho. Statistical analysis: Hyunsuk Kim, Yong Chul Kim, Ye Hyun Kim, Myung Kyu Lee, Hyun-Seok Min, and Hyungjoo Cho. Data analysis and interpretation: Jung Hyun Shin, Hyungjoo Cho, Hyunsuk Kim, Yong Chul Kim, Yong Seong Lee, and Tae Young Shin. Drafting of the manuscript: Jung Hyun Shin. Critical revision of the manuscript: Jung Hyun Shin and Tae Young Shin. Obtaining funding: Tae Young Shin. Administrative, technical, or material support: Tae Young Shin. Supervision: Yong Seong Lee and Tae Young Shin. Approval of the final manuscript: all authors.

SUPPLEMENTARY MATERIAL

Accompanying video can be found in the 'Urology in Motion' section of the journal homepage (www.icurology.org). The supplementary video clip can also be accessed by scanning a QR code, and will be available on YouTube: Supplementary Video, <https://youtu.be/gVh72uY2cSU>.



REFERENCES

1. Lanktree MB, Haghighi A, Guiard E, Iliuta IA, Song X, Harris PC, et al. Prevalence estimates of polycystic kidney and liver disease by population sequencing. *J Am Soc Nephrol* 2018;29:2593-600.
2. Grantham JJ, Torres VE, Chapman AB, Guay-Woodford LM, Bae KT, King BF Jr, et al. Volume progression in polycystic kidney disease. *N Engl J Med* 2006;354:2122-30.
3. Chapman AB, Devuyst O, Eckardt KU, Gansevoort RT, Harris T, Horie S, et al. Autosomal-dominant polycystic kidney disease (ADPKD): executive summary from a Kidney Disease: Improving Global Outcomes (KDIGO) Controversies Conference. *Kidney Int* 2015;88:17-27.
4. Müller RU, Messchendorp AL, Birn H, Capasso G, Cornec-Le Gall E, Devuyst O, et al. An update on the use of tolvaptan for autosomal dominant polycystic kidney disease: consensus statement on behalf of the ERA Working Group on Inherited Kidney Disorders, the European Rare Kidney Disease Reference Network and Polycystic Kidney Disease International. *Nephrol Dial Transplant* 2022;37:825-39.
5. Testa F, Magistroni R. ADPKD current management and ongoing trials. *J Nephrol* 2020;33:223-37.
6. Bae KT, Commean PK, Lee J. Volumetric measurement of renal cysts and parenchyma using MRI: phantoms and patients with polycystic kidney disease. *J Comput Assist Tomogr* 2000;24:614-9.
7. Bae KT, Tao C, Wang J, Kaya D, Wu Z, Bae JT, et al. Novel approach to estimate kidney and cyst volumes using mid-slice magnetic resonance images in polycystic kidney disease. *Am J Nephrol* 2013;38:333-41.
8. Sharbatdaran A, Romano D, Teichman K, Dev H, Raza SI, Goel A, et al. Deep learning automation of kidney, liver, and spleen segmentation for organ volume measurements in autosomal dominant polycystic kidney disease. *Tomography* 2022;8:1804-19.
9. Shin TY, Kim H, Lee JH, Choi JS, Min HS, Cho H, et al. Expert-level segmentation using deep learning for volumetry of polycystic kidney and liver. *Investig Clin Urol* 2020;61:555-64.
10. Park HC, Hong Y, Yeon JH, Ryu H, Kim YC, Lee J, et al. Mayo imaging classification is a good predictor of rapid progress among Korean patients with autosomal dominant polycystic kidney disease: results from the KNOW-CKD study. *Kidney Res Clin Pract* 2022;41:432-41.
11. Irazabal MV, Rangel LJ, Bergstralh EJ, Osborn SL, Harmon AJ, Sundsbak JL, et al. Imaging classification of autosomal dominant polycystic kidney disease: a simple model for selecting patients for clinical trials. *J Am Soc Nephrol* 2015;26:160-72.
12. Chebib FT, Torres VE. Assessing risk of rapid progression in autosomal dominant polycystic kidney disease and special considerations for disease-modifying therapy. *Am J Kidney Dis* 2021;78:282-92.
13. Onthoni DD, Sheng TW, Sahoo PK, Wang LJ, Gupta P. Deep learning assisted localization of polycystic kidney on contrast-enhanced CT images. *Diagnostics (Basel)* 2020;10:1113.
14. Sharma K, Rupprecht C, Caroli A, Aparicio MC, Remuzzi A, Baust M, et al. Automatic segmentation of kidneys using deep learning for total kidney volume quantification in autosomal dominant polycystic kidney disease. *Sci Rep* 2017;7:2049.
15. Kim Y, Bae SK, Cheng T, Tao C, Ge Y, Chapman AB, et al. Automated segmentation of liver and liver cysts from bounded abdominal MR images in patients with autosomal dominant polycystic kidney disease. *Phys Med Biol* 2016;61:7864-80.
16. Kline TL, Edwards ME, Fetzer J, Gregory AV, Anaam D, Metzger AJ, et al. Automatic semantic segmentation of kidney cysts in MR images of patients affected by autosomal dominant polycystic kidney disease. *Abdom Radiol (NY)* 2021;46:1053-61.
17. Kline TL, Korfiatis P, Edwards ME, Blais JD, Czerwiec FS, Har-

- ris PC, et al. Performance of an artificial multi-observer deep neural network for fully automated segmentation of polycystic kidneys. *J Digit Imaging* 2017;30:442-8.
18. van Gastel MDA, Edwards ME, Torres VE, Erickson BJ, Gansevoort RT, Kline TL. Automatic measurement of kidney and liver volumes from MR images of patients affected by autosomal dominant polycystic kidney disease. *J Am Soc Nephrol* 2019;30:1514-22.
 19. Raj A, Tollens F, Hansen L, Golla AK, Schad LR, Nörenberg D, et al. Deep learning-based total kidney volume segmentation in autosomal dominant polycystic kidney disease using attention, cosine loss, and sharpness aware minimization. *Diagnostics (Basel)* 2022;12:1159.
 20. Jagtap JM, Gregory AV, Homes HL, Wright DE, Edwards ME, Akkus Z, et al. Automated measurement of total kidney volume from 3D ultrasound images of patients affected by polycystic kidney disease and comparison to MR measurements. *Abdom Radiol (NY)* 2022;47:2408-19.
 21. Roudenko A, Mahmood S, Du L, Gunio D, Barash I, Doo F, et al. Semi-automated 3D volumetric renal measurements in polycystic kidney disease using b0-images-a feasibility study. *Tomography* 2021;7:573-80.
 22. Simms RJ, Doshi T, Metherall P, Ryan D, Wright P, Gruel N, et al. A rapid high-performance semi-automated tool to measure total kidney volume from MRI in autosomal dominant polycystic kidney disease. *Eur Radiol* 2019;29:4188-97.
 23. Isensee F, Jaeger PF, Kohl SAA, Petersen J, Maier-Hein KH. nnU-Net: a self-configuring method for deep learning-based biomedical image segmentation. *Nat Methods* 2021;18:203-11.
 24. Lanktree MB, Guiard E, Li W, Akbari P, Haghghi A, Iliuta IA, et al. Intrafamilial variability of ADPKD. *Kidney Int Rep* 2019;4:995-1003.
 25. Lavu S, Vaughan LE, Senum SR, Kline TL, Chapman AB, Perrone RD, et al. The value of genotypic and imaging information to predict functional and structural outcomes in ADPKD. *JCI Insight* 2020;5:e138724.
 26. Shoaf SE, Chapman AB, Torres VE, Ouyang J, Czerwiec FS. Pharmacokinetics and pharmacodynamics of tolvaptan in autosomal dominant polycystic kidney disease: phase 2 trials for dose selection in the pivotal phase 3 trial. *J Clin Pharmacol* 2017;57:906-17.
 27. Torres VE, Chapman AB, Devuyst O, Gansevoort RT, Perrone RD, Koch G, et al. Tolvaptan in later-stage autosomal dominant polycystic kidney disease. *N Engl J Med* 2017;377:1930-42.
 28. Torres VE, Chapman AB, Devuyst O, Gansevoort RT, Grantham JJ, Higashihara E, et al. Tolvaptan in patients with autosomal dominant polycystic kidney disease. *N Engl J Med* 2012;367:2407-18.